Behavioral/Cognitive

A Variable Oscillator Underlies the Measurement of Time Intervals in the Rostral Medial Prefrontal Cortex during Classical Eyeblink Conditioning in Rabbits

C. Rocío Caro-Martín, Rocío Leal-Campanario, Raudel Sánchez-Campusano, José M. Delgado-García, and Agnès Gruart

Division of Neurosciences, Pablo de Olavide University, Seville-41013, Spain

We were interested in determining whether rostral medial prefrontal cortex (rmPFC) neurons participate in the measurement of conditioned stimulus–unconditioned stimulus (CS-US) time intervals during classical eyeblink conditioning. Rabbits were conditioned with a delay paradigm consisting of a tone as CS. The CS started 50, 250, 500, 1000, or 2000 ms before and coterminated with an air puff (100 ms) directed at the cornea as the US. Eyelid movements were recorded with the magnetic search coil technique and the EMG activity of the orbicularis oculi muscle. Firing activities of rmPFC neurons were recorded across conditioning sessions. Reflex and conditioned eyelid responses presented a dominant oscillatory frequency of ≈12 Hz. The firing rate of each recorded neuron presented a single peak of activity with a frequency dependent on the CS-US interval (i.e., ≈12 Hz for 250 ms, ≈6 Hz for 500 ms, and≈3 Hz for 1000 ms). Interestingly, rmPFC neurons presented their dominant firing peaks at three precise times evenly distributed with respect to CS start and also depending on the duration of the CS-US interval (only for intervals of 250, 500, and 1000 ms). No significant neural responses were recorded at very short (50 ms) or long (2000 ms) CS-US intervals. rmPFC neurons seem not to encode the oscillatory properties characterizing conditioned eyelid responses in rabbits, but are probably involved in the determination of CS-US intervals of an intermediate range (250–1000 ms). We propose that a variable oscillator underlies the generation of working memories in rabbits.

Key words: **delay conditioning; neural oscillators; prefrontal cortex; rabbits; unitary recordings**

Significance Statement

The way in which brains generate working memories (those used for the transient processing and storage of newly acquired information) is still an intriguing question. Here, we report that the firing activities of neurons located in the rostromedial prefrontal cortex recorded in alert behaving rabbits are controlled by a dynamic oscillator. This oscillator generated firing frequencies in a variable band of 3–12 Hz depending on the conditioned stimulus–unconditioned stimulus intervals (1 s, 500 ms, 250 ms) selected for classical eyeblink conditioning of behaving rabbits. Shorter (50 ms) and longer (2 s) intervals failed to activate the oscillator and prevented the acquisition of conditioned eyelid responses. This is an unexpected mechanism to generate sustained firing activities in neural circuits generating working memories.

Introduction

Motor tremor should not be taken as an admonitory symptom of a pathological condition, as an unwanted byproduct of movement performance, or as the exclusive result of the inertial and viscoelastic properties of moving body parts, but rather as the necessary background for the coordinated execution of spontaneous and acquired movements (Llinás, 1991; Elble, 1996; Volkmann et al., 1996; Park et al., 2010; Louis, 2014). In a previous study of the kinematic properties of cat eyelids, Gruart et al. (1995) suggested the existence of a 20–25 Hz oscillator underlying reflex and classical eyeblink responses. Indeed, published records note the easily seen presence of oscillations in eyelid movements or in the EMG activity of involved facial or retractor bulbi muscle (Berthier, 1992; Welsh, 1992). In particular, eyelid oscillations in rabbits present a dominant frequency of 4–15 Hz (Gruart et al., 2000). It was shown previously that oscillatory

Received June 14, 2015; revised Sept. 15, 2015; accepted Sept. 29, 2015.

Author contributions: R.S.-C., J.M.D.-G., and A.G. designed research; C.R.C.-M., R.L.-C., R.S.-C., J.M.D.-G., and A.G. performed research; C.R.C.-M., R.L.-C., R.S.-C., J.M.D.-G., and A.G. analyzed data; J.M.D.-G. and A.G. wrote the paper.

This work was supported by the Spanish Ministry of Economy and Competitiveness (Grant BFU2014-56692-R to A.G. and J.M.D.-G.) and Junta de Andalucía (Grants BIO122, CVI 2487, and P07-CVI-02686 to A.G. and J.M.D.-G.). We thank Roger Churchill for help in manuscript editing.

The authors declare no competing financial interests.

Correspondence should be addressed to Prof. Agnès Gruart, Division of Neurosciences, Pablo de Olavide University, Ctra. de Utrera, Km. 1, Seville-41013, Spain. E-mail: agrumas@upo.es.

DOI:10.1523/JNEUROSCI.2285-15.2015

 0270-6474/15/3514809-13$15.00/0

activities of the eyelid are tuned to its size and viscoelastic properties, as determined in different (mouse, rat, rabbit, cat, and human) species of mammals (Domingo et al., 1997; Gruart et al., 2000; Koekkoek et al., 2002).

Oscillations in a range similar to those presented by the lids have also been described in the resting membrane potentials and firing properties of cat facial motoneurons (Trigo et al., 1999) and motor cortex neurons (Aou et al., 1992) during the performance of conditioned eyeblinks. In a recent study of the firing activities of rostral medial prefrontal cortex (rmPFC) neurons in rabbits during the classical conditioning of eyelid responses, we reported the presence of dominant peaks in the discharge rate of recorded neurons at different latencies with respect to CS presentations, but always within the CS-US interval (Leal-Campanario et al., 2013). This observation raised the possibility that neural firing of rmPFC neurons could be related to the oscillatory properties and timing of conditioned eyeblinks or, on the contrary, could be involved in the determination of CS-US intervals, associative strength of conditioning stimuli, or related matters.

We recorded the firing activities of rmPFC neurons during classical eyeblink conditioning of behaving rabbits. For conditioning, we used a delay because it has been reported that cerebral cortical areas are not involved in its proper acquisition and retrieval (Clark et al., 1984; Takehara-Nishiuchi et al., 2005; Oswald et al., 2006). In this way, we could determine whether rmPFC activity during this type of associative learning is engaged in additional neural processing of associative learning tasks. To properly determine the oscillatory properties of conditioned eyelid responses, lid movements were recorded with the magnetic search coil technique (Gruart et al., 2000). The EMG activity of the ipsilateral orbicularis oculi muscle was also recorded. Firing activities of contralateral pyramidal rmPFC neurons were recorded across the successive conditioning sessions. Collected results suggest that the rmPFC plays an important role in cognitive processes related to associative learning tasks, such as the determination of CS-US intervals. In contrast, the rmPFC does not seem to be involved directly in the acquisition process or in the execution of the acquired eyelid responses.

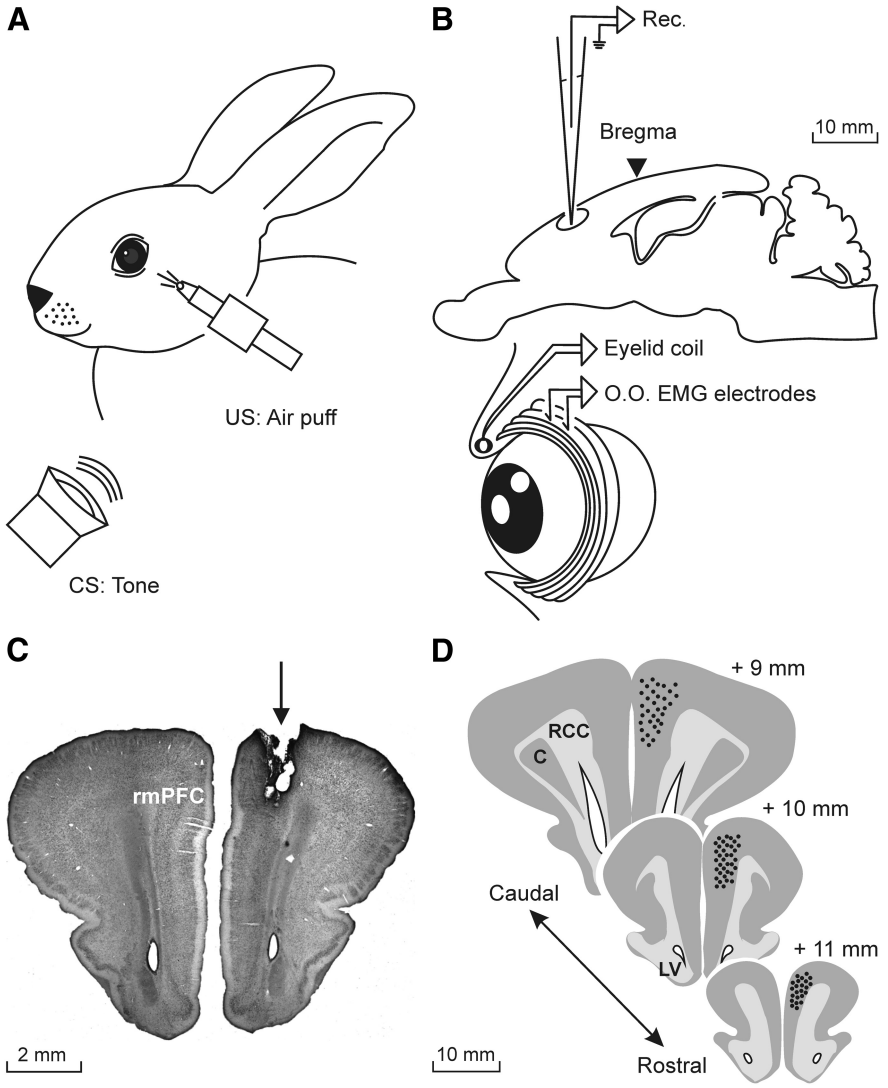

Figure 1. Experimental design. ***A***, For the classical conditioning of eyelid responses with a delay paradigm, rabbits were presented with a tone (600 Hz, 85 dB) as a CS. The tone was followed at different CS-US intervals (100, 250, 500, 1000, or 2000 ms) by an air puff (100 ms, 3 kg/cm^2) directed at the left cornea as a US. The two stimuli terminated simultaneously. ***B***, Diagram illustrating the rmPFC recording (Rec.) area. Eyelid movements were recorded using the magnetic field search coil technique with the help of a coil chronically implanted in the left upper lid. Animals were also implanted with EMG recording electrodes in the ipsilateral orbicularis oculi (O.O.) muscle. ***C***, Photomicrograph illustrating an electrolytic lesion (arrow) performed in the rmPFC recording sites. ***D***, Schematic diagrams in stereotaxic coordinates from rabbit brain with indication of the recording (black dots) sites. Calibrations for ***B***–***D*** are indicated. C, Claustrum; LV, lateral ventricle; RCC, corpus callosum.

Materials and Methods

Experimental animals. Experiments were performed on adult male rabbits (New Zealand white albino) weighing 2.5–3 kg on arrival obtained from an authorized supplier (Isoquimen). Animals were housed in individual cages for the whole experiment and kept on a 12/12 h light/dark cycle with constant ambient temperature (21 ± 1°C) and humidity (50 ± 7%). Food and water were available *ad libitum*. All experimental procedures were performed in accordance with European Union (2010/63/EU) guidelines and Spanish (BOE 34/11370-421, 2013) regulations for the use of laboratory animals in chronic experiments. Experimental protocols were also approved by the local University Ethics Committee.

Surgery. Animals were anesthetized with intramuscular injections of a ketamine–xylazine mixture (Ketaminol, 50 mg/ml; Rompun, 20 mg/ml; and atropine sulfate, 0.5 mg/kg). The anesthesia dosage was 0.35 ml/kg and was maintained by intravenous perfusion of the mixture at a flow rate of 10 mg/kg/h. As illustrated in Figure 1, all of the animals ($n = 24$) were implanted with a 5-turn coil (3 mm in diameter) into the center of the left upper eyelid close to the lid margin. Coils were made from Teflon-coated stainless steel wire (A-M Systems) with an external diameter of 50 μm and weight of 10–15 mg. Animals were also implanted with recording bipolar hook electrodes in the ipsilateral orbicularis oculi muscle. These electrodes were made from the same stainless steel wire. In addition, a 5 × 5 mm window was drilled in the frontal bone centered above the right rmPFC (Girgis and Shih-Chang, 1981; Shek et al., 1986). The dura mater was removed and an acrylic recording chamber was

constructed around the window. The brain surface was protected with a piece of silicone sheet and the chamber was filled with sterile gauze and capped with a plastic cover. A needle tip was implanted stereotaxically in one corner of the chamber for reference purposes during unitary recordings. Finally, a head-holding system consisting of three bolts cemented to the skull perpendicular to the stereotaxic plane was implanted. A silver electrode (1 mm in diameter) was attached to the skull as a ground. Terminals of the coil and EMG and ground electrodes were soldered to a six-pin socket. All wire connections were covered with cyanoacrylate glue and the whole system was attached to the skull with the aid of three small screws fastened and cemented with an acrylic resin to the bone (for details, see Leal-Campanario et al., 2007, 2013).

Recording and stimulation procedures. Recording sessions began 2 weeks after surgery. Each rabbit was placed in a Perspex restrainer specially designed for limiting the animal's movements (Gruart et al., 2000). The box was placed on the recording table and was surrounded by a black cloth. The recording room was kept softly illuminated and a 60 dB background white noise was switched on during the experiments. For all subjects, the first two recording sessions consisted of adapting the rabbit to the restrainer and to the experimental conditions; no stimulus was presented during these two sessions.

Eyelid movements were recorded with the magnetic field search coil technique (coil system from C-N-C Engineering). Eyelid coils were calibrated with a transparent protractor placed sagittally to the animal's head and with its center located at the external canthus of the lids. Eyelid closures were evoked with air puffs. Upper eyelid maximum opening ranged from 30° to 40° for the 24 animals. For the sake of homogeneity, the gain of the recording system was adjusted to yield 1 V per 10° (Gruart et al., 2000). The EMG activity of the orbicularis oculi muscle was recorded using a Grass P511 differential amplifier with a bandwidth of 0.1 Hz to 10 kHz.

Neuronal electrical activity was recorded in the rmPFC area with the help of a NEX-1 preamplifier (Biomedical Engineering). These recordings were performed with glass micropipettes filled with 2 M NaCl (3–6 MΩ of resistance) and filtered in a bandwidth of 1 Hz to 10 kHz. The recording area was approached with the help of stereotaxic coordinates (Girgis and Shih-Chang, 1981; Shek et al., 1986). At the end of each recording session, the recording micropipette was always removed and the recording chamber sterilized and closed.

Tones were applied from a loudspeaker located 80 cm below the animal's head. Air puffs directed at the left cornea were delivered through the opening of a plastic pipette (3 mm in diameter) attached to a metal holder fixed to the animal's nine-pin socket (dual-channel air-puff device; Biomedical Engineering).

Classical conditioning. Classical eyeblink conditioning was achieved by the use of a delay conditioning paradigm as described in detail previously (Leal-Campanario et al., 2007, 2013). For this, animals were presented with a tone (600 Hz, and 85 dB) as the CS, followed 50, 250, 500, 1000, or 2000 ms from its beginning by an air puff (100 ms, 3 kg/cm^2) as the US (Fig. 1*A*). The two stimuli terminated at the same time. Four animals were used for each of these five CS-US time intervals. The conditioning session consisted of 66 CS-US trials separated at random by intervals of 50–70 s. Six of the 66 trials were test trials in which the CS was presented alone. A conditioning session lasted for ≈70 min and animals were trained on 10 successive days. We considered a conditioned response (CR) the presence during the CS–US interval of EMG activity initiated >50 ms after CS onset and with a peak amplitude at least 2 times greater than the EMG amplitude recorded 50 ms before the CS onset. In addition, an animal was considered conditioned when it was able to produce 80% of CRs per session to the CS-US paired presentation (Gruart et al., 2000; Leal-Campanario et al., 2007, 2013). For the two habituation sessions, animals were presented with the CS alone for the same number of trials/session and at the same time intervals. Pseudoconditioning sessions, performed in four additional animals, also consisted of 66 trials separated at random by intervals of 50–70 s. For each trial, the CS was presented unpaired in relation to the US, the only restriction being that no more than two CS or US trials occurred sequentially (Gruart et al., 2000). The total training per session for pseudoconditioning was the same as for conditioning.

Unitary recordings in the rmPFC area were made during habituation, conditioning, and pseudoconditioning sessions (Fig. 1*B*). The recording micropipette was approached to the selected recording site with the help of the implanted reference needle. The recording site was changed in the horizontal plane in steps of 0.1 mm until a suitable unit was recorded and identified (Leal-Campanario et al., 2007, 2013; Pacheco-Calderón et al., 2012). Neuron isolation was performed during the time intervals in which CS-US pairs of stimuli were not presented. Usually, a range of 1–6 neurons was recorded per conditioning session.

Histology. At the end of the experiments, animals were deeply anesthetized with sodium pentobarbital (50 mg/kg, i.p.) and perfused transcardially with saline and 4% paraformaldehyde. The proper location of eyelid coil and EMG electrodes was checked. To determine the recording sites in the prefrontal cortex a small electrolytic lesion (CS-220 stimulator; Cibertec) was performed in all of the animals, their brain was removed and cut into slices (50 μm), and the relevant cortical areas were processed for Nissl staining (Fig. 1*C*). Recording sites were adjusted according to the collected stereotaxic coordinates and with the location of the electrolytic marks (Fig. 1*D*).

Data collection and analysis. The horizontal and vertical position of the upper eyelid, the unrectified EMG activity of the orbicularis oculi muscle, the unitary activity recorded in the rmPFC, and 1 V rectangular pulses corresponding to CS and US presentations were acquired online through an 8-channel analog-to-digital converter (1401-plus; CED), and transferred to a computer for quantitative offline analysis. Data were sampled at 5000 Hz (for EMG recordings) or 25000 Hz (for unitary recordings), with an amplitude resolution of 12 bits. Computer programs (Spike2 and SIGAVG from CED) were used to display eyelid position, velocity, and acceleration, as well as EMG and unitary activities (Figs. 2, 3). When necessary for quantitative analysis, segments containing CRs were selected exclusively from those obtained during the presentation of the CS alone. The programs also allowed the representation of the firing rate of the recorded neurons (Múnera et al., 2001; Leal-Campanario et al., 2007, 2013).

Velocity and acceleration traces were computed digitally as the first and second derivative of eyelid position records after low-pass filtering of the data (23 dB cutoff at 50 Hz and a zero gain at ≈100 Hz; Fig. 2*A*). As explained in detail previously (Domingo et al., 1997), the power of the spectral density function (i.e., the power spectrum) of selected data were calculated using a fast Fourier transform to determine the relative strength of the different frequencies present in eyelid displacements. The power spectra of eyelid movements were calculated exclusively from the corresponding acceleration (Domingo et al., 1997; Gruart et al., 2000). Acceleration segments (1.024 s) containing CRs were selected exclusively from those obtained during the presentation of the CS alone. This design allowed the complete CR to be contained in the segment with a spectral resolution of 0.97 Hz (Fig. 2*C*,*D*).

For unitary analysis, we designed and developed a customized spike-sorting algorithm called *VISSOR* (Viability of Integrated Spike Sorting of Real Recordings) on a MATLAB (The MathWorks) platform, which determined the number of neuronal spikes distributed across time with up to 22 physiological parameters characterizing each action potential (Fig. 3*A*,*B*; Porras-García et al., 2010; Caro-Martín et al., 2014, 2015). In short, a total of eight parameters of spike shapes in time domain (e.g., spike duration, peak-to-peak amplitude, negative and positive deflections), nine parameters from spike trajectory in phase space (e.g., negative and positive peaks of the first and second derivatives), and five parameters in relation to the distribution measures (e.g., interquartiles metrics, kurtosis coefficient, Fisher asymmetry) were determined from each recorded unit. Spikes were automatically grouped by *k*-means clustering (Paraskevopoulou et al., 2013), followed by an index of validation (e.g., silhouette) to verify the homogeneity and dissimilarity between spikes during classification (Su et al., 2013). For raster plots, we examined the firing-rate patterns (peak firing rate and time-locked firing) for all spiking events. Finally, we clustered the spiking events by means of an unsupervised procedure (hierarchical clustering analysis) of patterns rec-

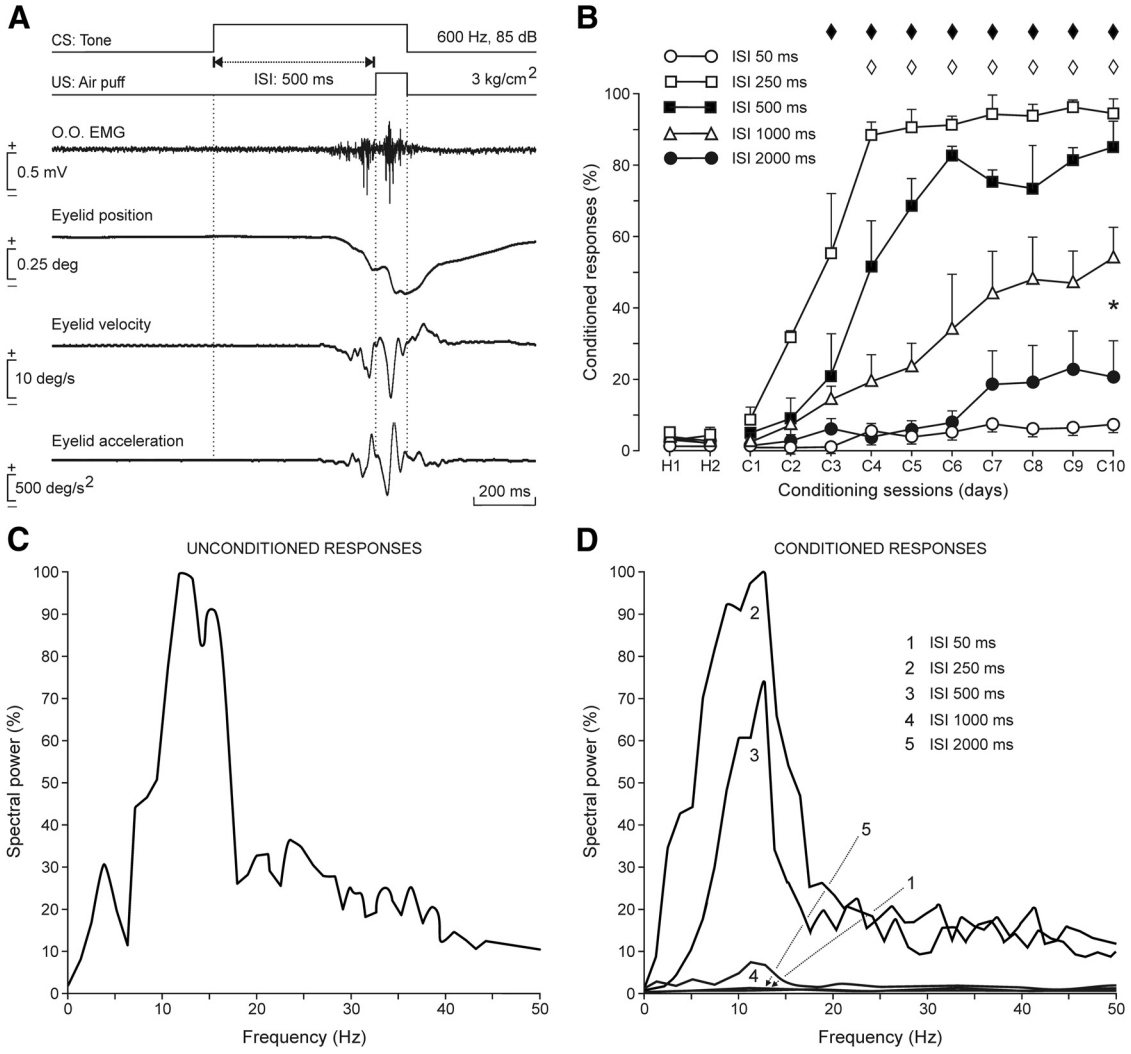

Figure 2. Frequency-component analysis for CRs as a function of CS-US intervals in a delay paradigm. ***A***, From top to bottom are illustrated the conditioning paradigm, representative examples of the EMG activity of the orbicularis oculi muscle (O.O. EMG), and eyelid position, velocity, and acceleration during the paired presentation of the CS followed 500 ms later by the US. ***B***, Evolution of the percentage of CRs (% CRs ± SEM) through the 10 conditioning sessions for five delay conditioning paradigms of different CS-US interval: 50 ms (○), 250 ms (□), 500 ms (■), 1000 ms (△), and 2000 ms (●). Note that animals conditioned with 250 or 500 ms CS-US intervals reached asymptotic values (80% of CRs) by the fourth to sixth conditioning sessions, but that those trained with the other three intervals failed to reach criterion by the 10th conditioning session. Data collected for intervals of 250 and 500 ms were not statistically different, but were significantly (one-way ANOVA on ranks, $p = 0.17$) different from those conditionings performed with the other three CS-US intervals. Pairwise multiple-comparison analysis, Holm–Sidak method: ♦ $p < 0.001$ for □ versus ○, △, and ●. ◊ $p < 0.001$ for ■ versus ○, △, and ●. *$p < 0.001$ for △ versus ○ and ●. ***C***, Illustration of the mean spectral power from ≥30 acceleration records ($n = 4$ rabbits) of eyelid reflex responses to air puffs (100 ms, 3 kg/cm^2) presented to the ipsilateral cornea. The 100% value for the illustrated spectral power corresponded to 0.93×10^7 (deg/s^2)^2, with a peak frequency of 12 Hz. ***D***, Mean spectral powers (≥10 acceleration profiles) of CRs evoked during the five different CS-US intervals illustrated in ***B*** (1, 50 ms; 2, 250 ms; 3, 500 ms; 4, 1000 ms; 5, 2000 ms). Each mean spectral power was obtained from two different rabbits. The 100% value for the illustrated spectral power corresponded to 0.3×10^7 (deg/s^2)^2. Peak frequencies for the different CS-US intervals were ≈12 Hz.

ognition and averaged the firing rate with similar time-locked firing and peak firing rates.

The spectral power of overlapped firing rate profiles was calculated by fitting a waveform with the help of the equation $f(t) = \alpha_0 \cos(wt)$, where α_0 is the mean value of the three dominant peaks in the averaged firing rates. Each waveform was calculated for the angular frequency $w = 2\pi/T$ where T is the average of the latency between the firing rate peaks with respect to CS presentation. The value of T was determined for each CS-US interval after the analysis of recorded firing rate profiles (Figs. 4, 5).

Computed results were processed for statistical analysis using the Statistics MATLAB Toolbox and SigmaPlot 11.0 package. As statistical inference procedures, both one- and two-way ANOVA (estimate of within-group and between-group variance on the basis of one dependent measure) and MANOVA (estimate of variance in multiple dependent parameters across groups) were used to assess the statistical significance of differences between groups. When the normality (Shapiro–Wilk or Kolmogorov–Smirnov tests) and equal variance of the errors (Levene Median test) assumptions were satisfied, the corresponding statistical significance test [i.e., the $F_{[(m-1),\,(m-1)\times(n-1),\,(l-m)]}$ statistics and the resulting probability $P < p$ at the predetermined significance level $p < 0.05$] was performed with sessions as repeated measures and coupled with contrast analysis when appropriate. The orders m (number of groups), n (number of rabbits), and l (number of multivariate observations) were reported accompanying the F-statistic values (Sánchez-Campusano et al., 2007). When the normality assumption was not confirmed, the significance (p value) of the χ^2 statistic was calculated using the ranks of the data rather than their numeric values. ANOVA test on ranks is a nonparametric version of the classical ANOVA F test and an extension of the Wilcoxon rank-sum test to more than two groups.

Wilk's lambda criterion and its transformation to the χ^2 distribution (MATLAB) were used to extract significant differences from MANOVA

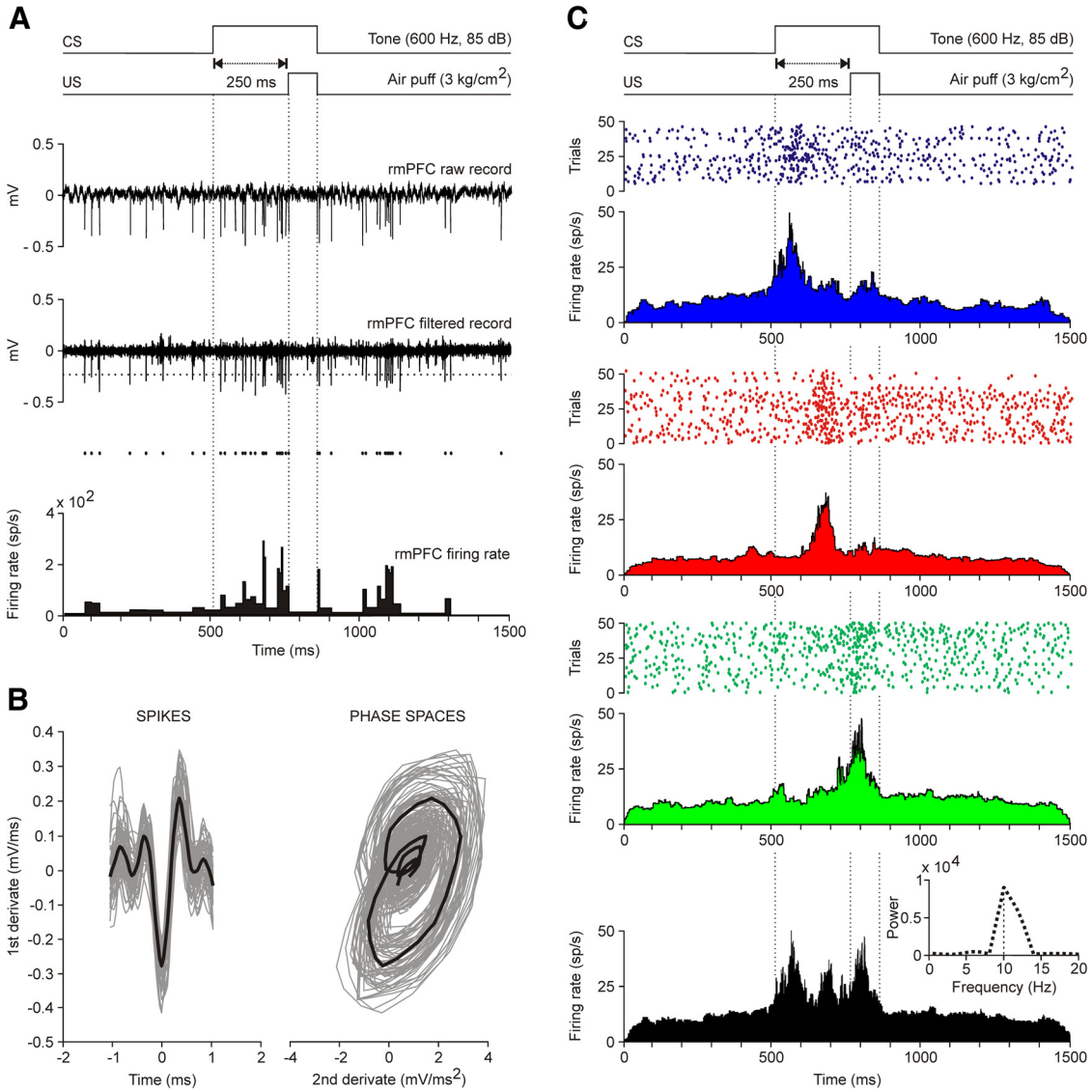

Figure 3. Firing activities of rmPFC neurons during classical eyeblink conditioning using a delay conditioning paradigm. ***A***, From top to bottom are illustrated a delay conditioning with indication of CS and US presentations. Below are illustrated the raw and filtered activity of a representative neuron collected during the ninth conditioning session, as well as a representation of its firing rate. The horizontal dotted line indicates the selected threshold. ***B***, At the left is represented a selection of the spikes detected by the selected threshold, while the phase space portraits (PSPs) of spike waveforms are represented at the right. Black traces indicated the mean value for each representation. ***C***, Representative examples of three different types of firing rate recorded during classical eyeblink conditioning. All of the illustrated raster displays were collected during the ninth conditioning session and were averaged from ≥40 trials. The three different firing rates were characterized by having their maximum frequency peaks close to the beginning of the CS (blue raster and firing rate, time to peak 59.4 ms, maximum frequency 46.35 spikes/s), in the center of the CS-US (red, time to peak 184.3 ms, maximum frequency 36.99 spikes/s), or next to the end of the US (green, time to peak 302.04 ms, maximum frequency 47.75 spikes/s). The black profile illustrates the overlap of the three firing rates shown above. The inset at the bottom right illustrates the spectral power [10^4(spikes/s)^2, peak frequency of 9.93 Hz] of the black profile. This spectrum was obtained by fitting a waveform with angular frequency $w = 2\pi/T$, where T is the average of the latency between the firing rate peaks with respect to CS presentation ($T = 100.68$ ms).

results (cluster analysis for cells–classes–spikes classification) during the spike-sorting problem in the phase space (Porras-García et al., 2010). Unless otherwise indicated, data are represented by the mean ± SEM.

Results

Oscillatory properties of reflex and classically conditioned eyelid responses

As illustrated in Figure 1, *A* and *B*, animals were prepared for the chronic recording of the EMG activity of the orbicularis oculi muscle and of eyelid movements with the help of the magnetic search coil technique. In Figure 2*A* is shown a representative example of reflex and conditioned eyelid responses during the eighth conditioning session recorded with the EMG electrodes and the coil implanted in the upper lid. Position, velocity, and acceleration profiles of the evoked eyelid responses are also illustrated. Air-puff-induced blinks consisted of a fast downward movement of the upper eyelid, followed by a much slower upward phase until the eyelid's initial position was reached (Fig. 2*A*). Mean latency of eyeblinks elicited by 100 ms, 3 kg/cm^2 air puffs was 19.5 ± 4.2 ms (mean ± SD; $n = 20$). The initial downward phase of evoked eyeblinks presented successive small sags in the direction of closure easily detected in the lid velocity and acceleration profiles. A power spectrum analysis was performed to determine the frequency components of the successive downward waves of air-puff-evoked blinks. The mean power spectra of 30 acceleration records from air-puff-evoked blinks collected from four rabbits showed a dominant peak at 12.6 ± 0.9 Hz over

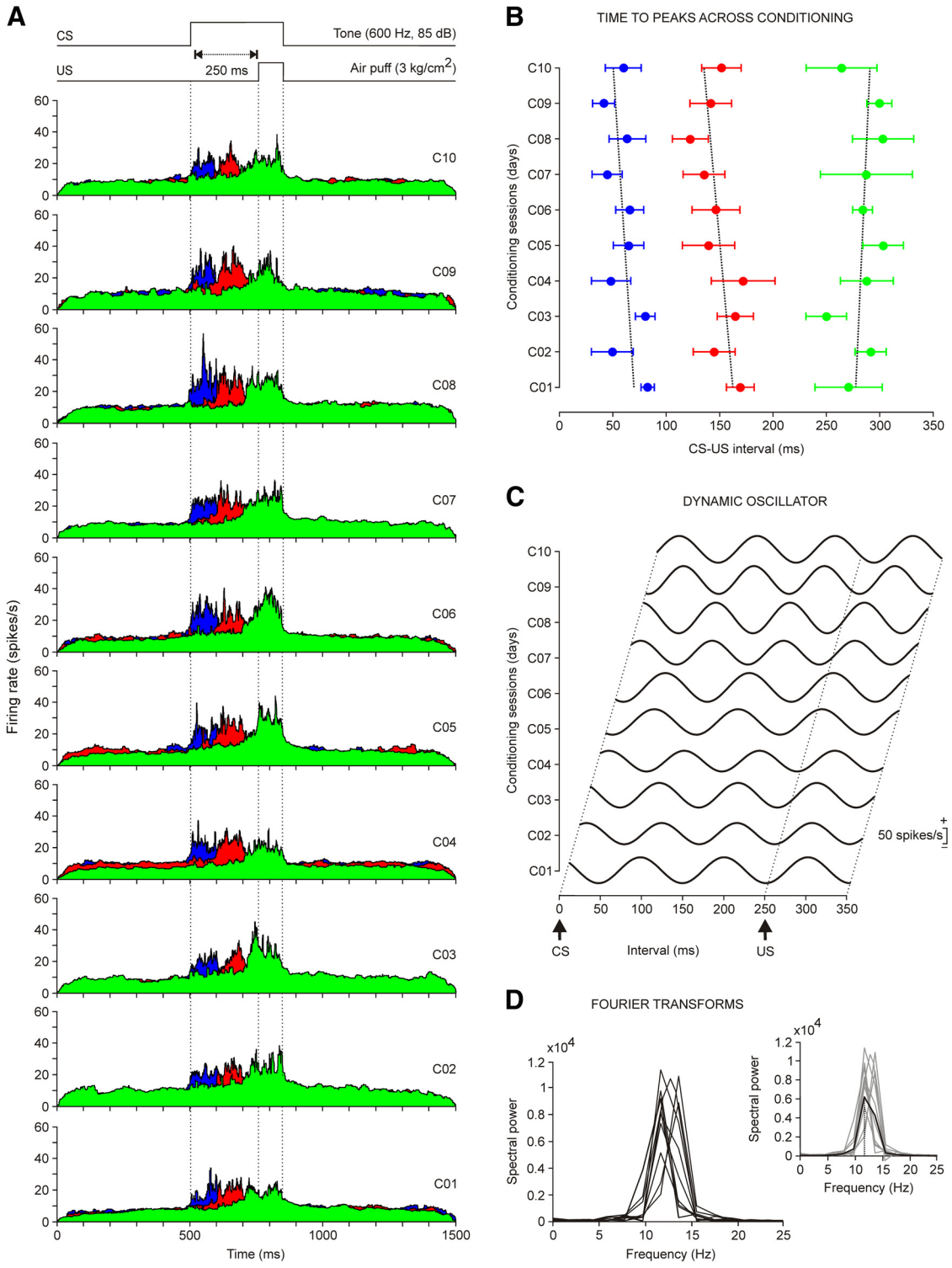

Figure 4. Evolution of the firing rate of rmPFC neurons across conditioning sessions with 250 ms of CS-US interval. ***A***, Firing rates of rmPFC neurons recorded from the first (C01) to the tenth (C10) conditioning sessions. Each illustrated profile was averaged from at least two neurons collected from four different animals. As in Figure 3*C*, the color code indicates the different peak latencies with respect to CS onset of the averaged firing rates. The conditioning paradigm is illustrated at the top. ***B***, Latency evolution for peak firing rates of the three different types of neuron across the 10 conditioning sessions. The corresponding regression lines were as follows: blue group, $y = -2.15x + 71.7$; red group, $y = -3.00x = 165.1$; and green group, $y = -1.47x + 275.7$. ***C***, Dynamic oscillator modeling firing rates. The oscillating curves were computed by fitting a waveform with an angular frequency $w = 2\pi/T$, where T is the average of the latency between the three dominant peaks with respect to CS presentation across the 10 conditioning sessions. The scale (in spikes/s) indicates mean firing rates. ***D***, Spectral powers obtained from the 10 oscillating curves illustrated in ***C***. On the right is shown the average from these 10 spectral powers. The average presented a maximum power of 0.6×10^4(spikes/s)^2 and a dominant frequency of 11.72 Hz.

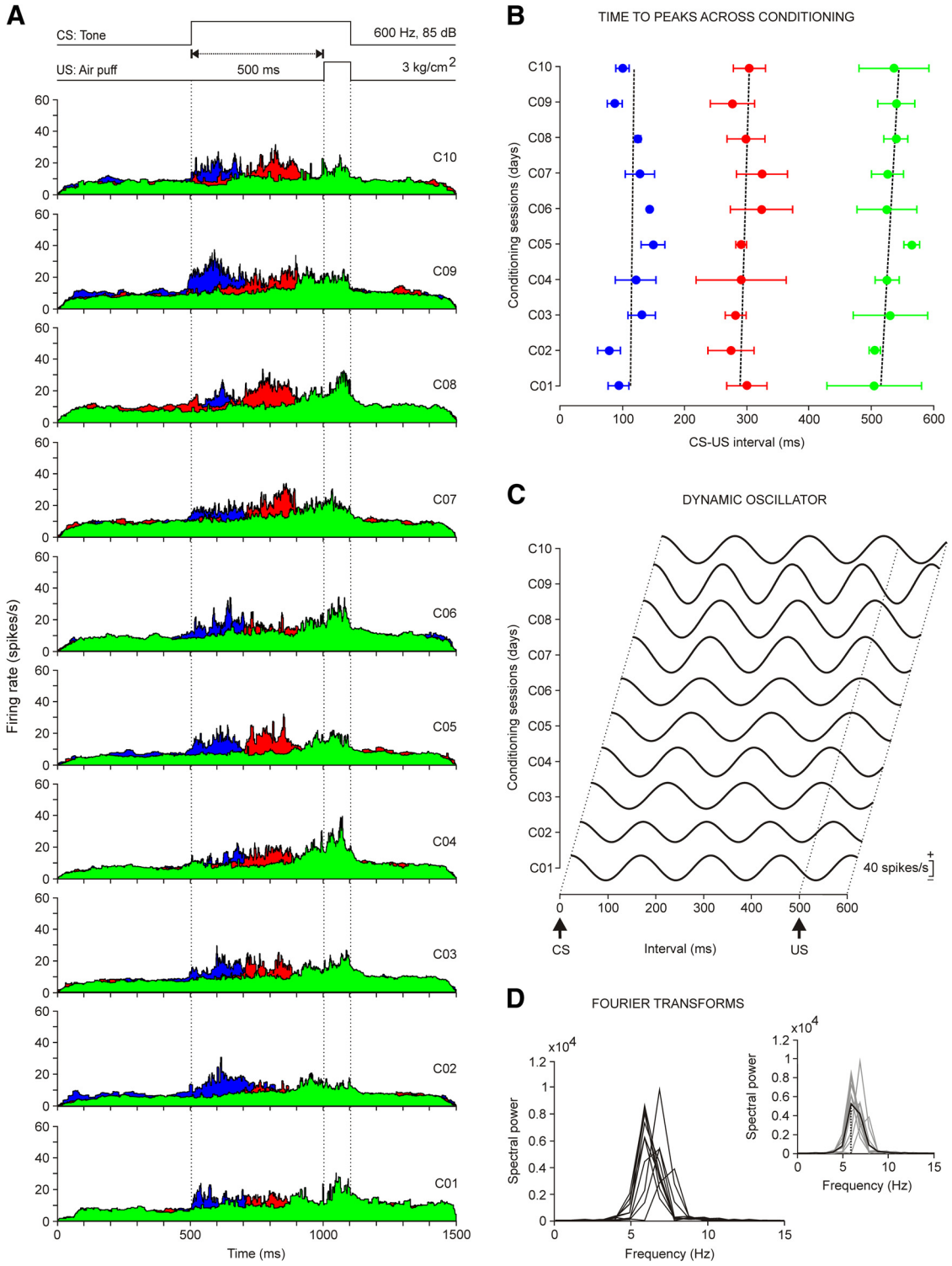

Figure 5. Evolution of the firing rate of rmPFC neurons across conditioning sessions with 500 ms of CS-US interval. ***A***, Firing rates of rmPFC neurons recorded from the first (C01) to the tenth (C10) conditioning sessions. Each illustrated profile was averaged from ≥2 neurons collected from four different animals. As shown in Figure 3*C*, the color code indicates the different peak latencies with respect to CS onset of the averaged firing rates. Note the progressive definition of the three types of firing rate during CS-US intervals. ***B***, Latency evolution for peak firing rates of the three different types of neuron across the 10 conditioning sessions. The corresponding regression lines were as follows: blue group, $y = 0.65x + 111.9$; red group, $y = 1.64x + 287.3$; and green group, $y = 3.22x + 511.9$. ***C***, Dynamic oscillator modeling firing rates. The oscillating curves were computed by fitting a waveform with an angular frequency $w = 2\pi/T$, where T is the average of the latency between the three dominant peaks with respect to CS presentation across the 10 conditioning sessions. The scale (in spikes/s) indicates mean firing rates. ***D***, Spectral powers were obtained from the curves illustrated in ***C***. On the right is shown the average from these 10 spectral powers. The average presented a maximum power of 0.54×10^4 (spikes/s)^2 and a dominant frequency of 5.86 Hz.

a broad band of frequencies between 7 and 17 Hz (Fig. 2*C*). This dominant oscillation for reflexively evoked blinks was slightly faster than that reported in a previous study, also in rabbits (4–15 Hz; Gruart et al., 2000).

Provided that all other characteristics of CS and US were maintained constant (see Materials and Methods), the percentage, profiles, and oscillatory properties of conditioned eyelid responses were highly dependent on CS-US intervals. Animals ($n = 4$) conditioned with a CS-US interval of 250 ms evoked >50% of CRs by the third conditioning session and reached asymptotic values (> 80% of CRs) by the fourth or fifth conditioning session (Fig. 2*B*). Onset latency of CRs evoked at this CS-US interval decreased through the successive conditioning sessions from 230.3 ± 19.3 ms for the first conditioning session to 118.6 ± 18.3 ms for the 10th. As described previously (Gruart et al., 2000), evoked conditioned eyelid responses also presented characteristic oscillatory profiles, but with accelerations 1/3 to 1/5 smaller than those reached by reflex eyeblinks (Fig. 2*A*). However, the spectral analysis of frequency components of conditioned eyelid responses evoked with CS-US intervals of 250 ms presented a significant peak at 11.8 ± 0.3 Hz— i.e., similar to that presented by reflexively evoked eyeblinks (Fig. 2*C*,*D*).

It was shown years ago that the optimal CS-US intervals for classical conditioning of nictitating membrane responses in rabbits ranged from 200 to 500 ms (Gormezano et al., 1983). In agreement with this early study, animals conditioned here with a CS-US interval of 500 ms achieved learning curves slightly lower than those presented by animals conditioned with an interstimulus interval of 250 ms (Fig. 2*B*). In contrast, animals conditioned with smaller (50 ms) or larger (1000 or 2000 ms) CS-US intervals presented learning curves significantly (one-way ANOVA on ranks; $p = 0.170$) lower than those of animals trained with CS-US intervals of 250 or 500 ms (Fig. 2*B*). In fact, animals trained with interstimulus intervals of 50 or 2000 ms did not reach the selected criterion (>40% of CRs by the 10th conditioning session) for the proper acquisition of this type of associative learning task.

Because the amplitude, velocity, and acceleration of conditioned eyelid responses was dependent on the selected CS-US interval (not illustrated), their respective spectral powers should also be different. Indeed, and as illustrated in Figure 2*D*, the spectral powers of conditioned eyeblinks evoked at CS-US intervals of 250 and 500 ms were significantly ($p \geq 0.01$) larger than values reached with the other three interstimulus intervals, but not different (one-way ANOVA F test; $F_{(1,1,10)} = 0.391$, $p = 0.546$) from one another. Interestingly, the dominant frequency was the same (≈12 Hz) in the other three cases (Fig. 2*D*). The scarce number of CRs (<10%) evoked during conditioning with 50 and 2000 ms of CS-US interval was too small to present any significant peak in the frequency domain (Fig. 2*D*). Pseudoconditioned animals did not present any identifiable CR.

On the whole, and consisent with previous reports in rabbits (Gruart et al., 2000) and cats (Domingo et al., 1997), conditioned eyelid responses evoked in behaving rabbits with classical conditioning procedures using delay paradigms of increasing CS-US interval can be characterized by an ≈12 Hz oscillation that is also present in reflexively evoked blinks. The next step was to determine whether these oscillatory properties could also be identified in the firing activities of rmPFC neurons.

Identification of rmPFC recorded neurons

As illustrated in Figure 1*B*, animals were prepared for unitary recordings in the rmPFC area. The histological examination of the recording sites indicated that the studied area was restricted to the rmPFC (AP = 9–11 mm, L = −1 mm, and D = 2.1–3.8 mm from bregma; Girgis and Shih-Chang, 1981; Shek et al., 1986), corresponding to the rostral aspect of Brodman's area 24 or anterior cingulate cortex and to the rostrodorsal part of Brodman's area 32 or prelimbic cortex (Fig. 1*C*,*D*). Previous histological studies (Benjamin et al., 1978; Leal-Campanario et al., 2007, 2013) have shown that this prefrontal area can be further identified by the preferential projections reaching it from the medial half of the mediodorsal thalamic nucleus.

In Figure 3*A* is illustrated an example of unitary recording in the rmPFC area during delay conditioning using a CS-US interval of 250 ms. For proper isolation and identification, recorded units were filtered, isolated, classified, and prepared for raster displays and the representation of their firing rates. The spike-sorting tools used here enabled the proper identification of the recorded unit (Fig. 3*B*). Only units with spike duration of >0.5 ms were considered pyramidal cells and further analyzed. The spontaneous firing rate of recorded cells ranged from 2 to 15 spikes/s. Characteristically, they presented spontaneous irregular bursts of activity that were similar in duration and profile to those presented by the recorded neurons across conditioning sessions. Because of their firing properties, most of the neurons analyzed here look similar to the regular-spiking, slow-adapting pyramidal cells described by Dégenètais et al. (2002)—namely, they were capable of generating a tonic firing restricted to a part of the CS-US interval in the presence of conditioned eyelid responses. Spike-triggered averaging ($n \geq 3000$ spikes) of recorded neurons did not evoke any identifiable activity in the EMG of the orbicularis oculi muscle, indicating the polysynaptic nature of rmPFC projections to facial motoneurons (not illustrated).

Firing properties of rmPFC neurons during classical eyeblink conditioning with a delay paradigm of 250 ms of CS-US interval

In Figure 3*C* are shown representative examples of three different types of rmPFC neuron recorded during delay conditioning with a CS-US interval of 250 ms. Recordings were performed during the ninth conditioning session and the three illustrated neurons were collected from two different animals. Although, according to their raster displays (>40 trials) and their averaged firing rates, the spontaneous firing of the three neurons was fairly similar, they presented a significant peak of activity at different moments of the CS-US interval. Therefore, in blue is represented the raster display and the firing rate of a neuron presenting a peak (≈45 spikes/s) of firing ≈60 ms after CS onset; in red is represented another neuron with a peak (≈37 spikes/s) of firing that happened ≈185 ms after CS presentation; finally, in green is represented a third neuron with a peak (≈48 spikes/s) of firing that happened ≈300 ms after CS presentation.

The firing rate in black illustrated in the bottom part of Figure 3*C* corresponds to the superimposition of the three colored firing rates illustrated above in the same figure. It should be noted that the three peaks of frequency took place during the CS presentation. A spectral analysis of these overlapping peaks of activity showed that peaks took place with a dominant frequency of ≈10 Hz (Fig. 3*C*, inset, bottom); that is, a value quite close to the dominant frequency (≈12 Hz) characteristic of reflex and conditioned eyelid responses (Fig. 2*A*,*C*,*D*).

In Figure 4*A* are illustrated the averaged firing rates of neurons recorded across the 10 sessions of a delay conditioning using a CS-US interval of 250 ms. Each represented colored average corresponds to ≥2 neurons recorded from the four animals included in this group. It is important to note that not a single neuron

presented more than one well defined peak (lasting from 80 to 140 ms) of frequency during the CS-US interval or that, as already shown (Leal-Campanario et al., 2013), none of them ($n = 95$ neurons, $n = 4$ rabbits) presented a sustained firing rate for the whole duration of the interstimulus interval. In contrast, there was a progressive improvement in the definition of the firing peaks across the successive training sessions (see below). In Figure 4*B* is represented the evolution in the latency of the three peaks present in the firing rate of the analyzed neurons (first peak, 29 neurons; second peak, 28 neurons; third peak, 38 neurons). As shown, no significant changes in latency with respect to CS onset were observed across conditioning sessions. In Figure 4*C* are represented 10 waveforms fitted to the three dominant peaks in frequency collected for each conditioning session. Note that the amplitude of the fitted waveforms increased with training—a fact reflected by the different powers of spectra illustrated in Figure 4*D*. In all cases, the average of the fast Fourier analysis of the 10 computed waveforms indicated the presence of a dominant frequency of 12.3 ± 0.3 Hz (Fig. 4*D*, inset).

These results prompted us to use a longer (500 ms) CS-US interval for classical conditioning to either confirm or rule out that the averaged firing of selected rmPFC neurons oscillates at a frequency independent of the interstimulus interval, as already shown for conditioned eyelid responses (Fig. 2*D*).

Firing properties of rmPFC neurons during classical eyeblink conditioning with a delay paradigm of 500 ms of CS-US interval

In Figure 5*A* are illustrated the averaged firing rates of neurons recorded across the 10 sessions of a delay conditioning using a CS-US interval of 500 ms. Each represented colored average corresponds to ≥2 neurons recorded from the four animals included in this group. Note that the dominant peaks present in the firing rates of neurons recorded during this conditioning task seem to adapt to the longer CS-US interval. Therefore, the duration of the peak increased ≈150% (120–200 ms) with respect to peak duration for the 250 ms interstimulus interval (80–140 ms). However, none of the recorded neurons ($n = 67$ neurons, $n = 4$ rabbits) presented a sustained firing rate for the whole duration of the interstimulus interval. In Figure 5*B* is represented the evolution in the latency of the three peaks present in the firing rate of the analyzed neurons (first peak, 18 neurons; second peak, 21 neurons; third peak, 28 neurons). As shown, no significant changes in latency with respect to CS onset were observed across conditioning sessions. In Figure 5*C* are represented 10 waveforms fitted to the three dominant peaks in frequency collected for each conditioning session. Note that the amplitude of the fitted waveforms increased with training, a fact reflected in the different powers of spectra illustrated in Figure 5*D*. In this case, the average of the fast Fourier analysis of the 10 computed waveforms indicated the presence of a dominant frequency of 6.2 ± 0.2 Hz (Fig. 5*D*, inset).

Consistent with the above results, the oscillatory properties of rmPFC neurons do not seem to be related to the dominant frequency of reflex and conditioned eyeblinks (i.e., 12 Hz), but do seem to be more related to CS-US intervals (≈12 Hz for 250 ms and ≈6 Hz for 500 ms). These results suggested that changes in the firing rate of rmPFC neurons could encode the duration of the selected time window and not the oscillatory properties of rabbit eyelids. Indeed, determining the duration of the CS-US interval could be important for the proper timing of the conditioned eyelid response. The difficulty to acquire conditioned eyelid responses with very short or very long CS-US (i.e., shorter or longer than 200–500 ms) has been reported repeatedly (Gormezano et al., 1983; Gruart et al., 1995, 2000).

Dependence of the oscillatory properties of rmPFC neurons on CS-US intervals

In Figure 6 are shown representative examples of averaged rmPFC neurons (≥2 collected from ≤4 animals). Recordings were performed during the eighth session of delay conditioning of different (50, 250, 500, 1000, and 2000 ms) CS-US intervals. The illustrated data show that peak firing rates of the averaged neurons occupy the CS-US interval in a definite form for 250 and 500 ms of interstimulus interval. The firing peaks of the three types of neuron ($n = 55$, $n = 4$ animals) were not so well defined for the 1000 ms CS-US interval (first peak, 17 neurons; second peak, 15 neurons; third peak, 23 neurons). Finally, neurons were nonresponding to CS-US presentations for the shortest (50 ms; $n = 41$ neurons, $n = 4$ rabbits) and the longest (2000 ms; $n = 43$ neurons, $n = 4$ rabbits) interstimulus interval. In addition, the spectral analysis indicated that the dominant frequency of the peaks in firing rate during the CS-US interval presented an inverse relationship with the interstimulus interval: 11.72 Hz for 250 ms, 5.86 for 500 ms, 2.9 Hz for 1000 ms, and 1.5 Hz for 2000 Hz. A summary of the collected results is shown in Figure 7. The mean spectral power corresponding to the different timing of peak firing rates as a function of the CS-US interval (Fig. 7*A*). It can be observed that both the power of each oscillation and its frequency decreased with the interstimulus interval (Fig. 7*B*). In contrast, although the amplitude of acceleration profiles collected from eyelid CRs for the different CS-US intervals decreased with their duration (Fig. 7*D*), the dominant frequency (≈12 Hz) remained unchanged (Fig. 7*C*).

Discussion

Main findings of the present study

Consistent with the present results, the rmPFC cortex could be involved in the determination of CS-US intervals, but as described previously (Leal-Campanario et al., 2013) and confirmed here, it is not directly involved in the acquisition process and/or in the proper execution of conditioned eyelid responses. Indeed, the discharge rate of rmPFC neurons was not related to the fixed oscillatory properties of rabbit eyelids, but modified their oscillation as a function of CS-US intervals. The more-definite oscillations presented by the rmPFC during CS-US intervals lasting for 250 and 500 ms could explain why these intervals are optimal for classical eyeblink conditioning (Gormezano et al., 1983; Gruart et al., 1995). Therefore, and in addition to the permissive/modulating role of the rmPFC in the rabbit for the generation of newly acquired motor responses (Leal-Campanario et al., 2007, 2013), rmPFC neurons could play an important role in the rabbit's ability regarding the temporal association between the CS and the US. Conversely, the determination of CS-US intervals by rmPFC neurons took place by the participation of three different types of neuron (characterized by their latency of activation to CS presentation). These results are in contrast with the persistent firing activity of other types of prefrontal neuron. For example, dorsolateral prefrontal cortex neurons show firing activities that persist during the CS-US interval in trace conditioning paradigms, helping in the generation of timed CRs (Weiss and Disterhoft, 2011). In addition, the specific population of caudal mPFC neurons recorded in rabbits also seems to bridge the temporal gap between the end of the CS and the beginning of the US during trace conditioning (Siegel et al., 2012). Therefore, as described previously (Powell et al., 2005), the firing of medial PFC

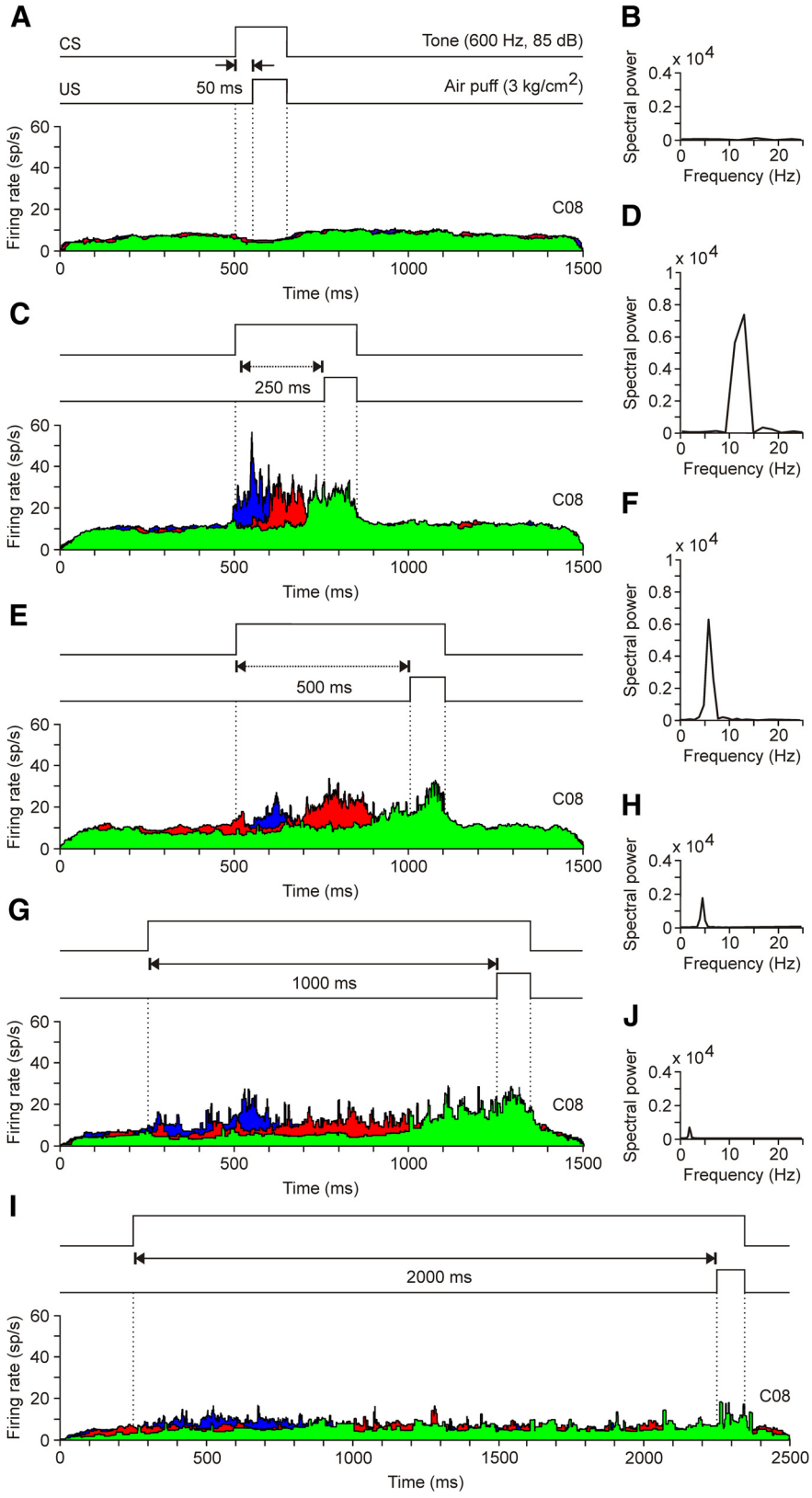

Figure 6. A comparison of the firing rates of rmPFC neurons presented during the five different CS-US intervals. ***A***, ***C***, ***E***, ***G***, ***I***, Representation of the three dominant firing rates collected during the eighth conditioning session (C08) for the five CS-US intervals used in this study. ***B***, ***D***, ***F***, ***H***, ***J***, Spectral powers of waveforms computed from the average of the latency between the peaks with respect to CS presentation (Figs. 4*C* and 5*C*). ***A***, ***B***, Note that, for this CS-US interval (50 ms), there was no activation of rmPFC neurons. ***C***, ***D***, For CS-US intervals of 250 ms, the firing rate of recorded rmPFC neurons presented a dominant frequency of 11.72 Hz [maximum power of 0.73×10^4 (spikes/s)^2]. ***E***, ***F***, In the case of CS-US intervals of 500 ms, the dominant frequency of the firing rate of rmPFC neurons went down to 5.86 Hz [maximum power of 0.59×10^4(spikes/s^2)]. ***G***, ***H***, For CS-US intervals of 1000 ms, the spectral power of the curve fitted to peak firing rates of recorded rmPFC neurons was reduced to 0.21×10^4(spikes/s)^2 and to a peak frequency of 2.9 Hz. ***I***, ***J***, The firing rate of rmPFC neurons presented a weak modulation for classical eyelid conditioning using a CS-US interval of 2000 ms. The spectral power of the curve fitted to peak firing rates was very low [0.09×10^4 (spikes/s)^2] and the peak frequency was 1.5 Hz.

neurons is not directly related to the acquisition of classical eyeblink conditioning. Consistent with this latter point, the rmPFC of subprimates is considered to be the highest level of the limbic system, as part of the orbital prefrontal cortex, and therefore involved in the accurate activation or inhibition of selected behaviors and of attentive and cognitive processes (Fuster, 2001, 2008; Kolb et al., 2004). This is probably the first report on the presence of a neural oscillator underlying the determination of time intervals during associative learning tasks, a neural process that has not been described for neurons located in the same medial prefrontal areas in primates (Fuster, 2008). This neural mechanism could also underlie the generation of hippocampal time cells (Eichenbaum, 2014; Howard and Eichenbaum, 2015).

Oscillatory properties of the eyelid motor system

The fact that reflex and conditioned nictitating membrane responses present a wavy profile was reported years ago (Berthier, 1992; Welsh, 1992) and was even observed in early classical conditioning experiments in humans (Marquis and Porter, 1939). Illustrations of reflex and conditioned nictitating membrane responses in those previous reports (Berthier, 1992; Welsh, 1992) show noticeable oscillations at 8–10.5 Hz, a value similar to the ≈8 Hz reported for eyelid movements in conditioned rabbits (Gruart et al., 2000) and close to values collected here (≈12 Hz). The dominant frequency of eyelid responses in the rabbit is ~1/3 of its resonant frequency (30–35 Hz; see Evinger et al., 1984), a finding also seen in cats (Domingo et al., 1997).

As already reported for finger movements in humans (Wessberg and Vallbo, 1995) and further confirmed here (Fig. 7*D*), larger CRs in rabbits and cats are achieved by increasing the amplitude and number of waves composing them, but not by modifying the dominant frequency of the movement (Domingo et al., 1997; Gruart et al., 2000). Therefore, the generation of a properly timed conditioned eyelid response could be envisioned as the

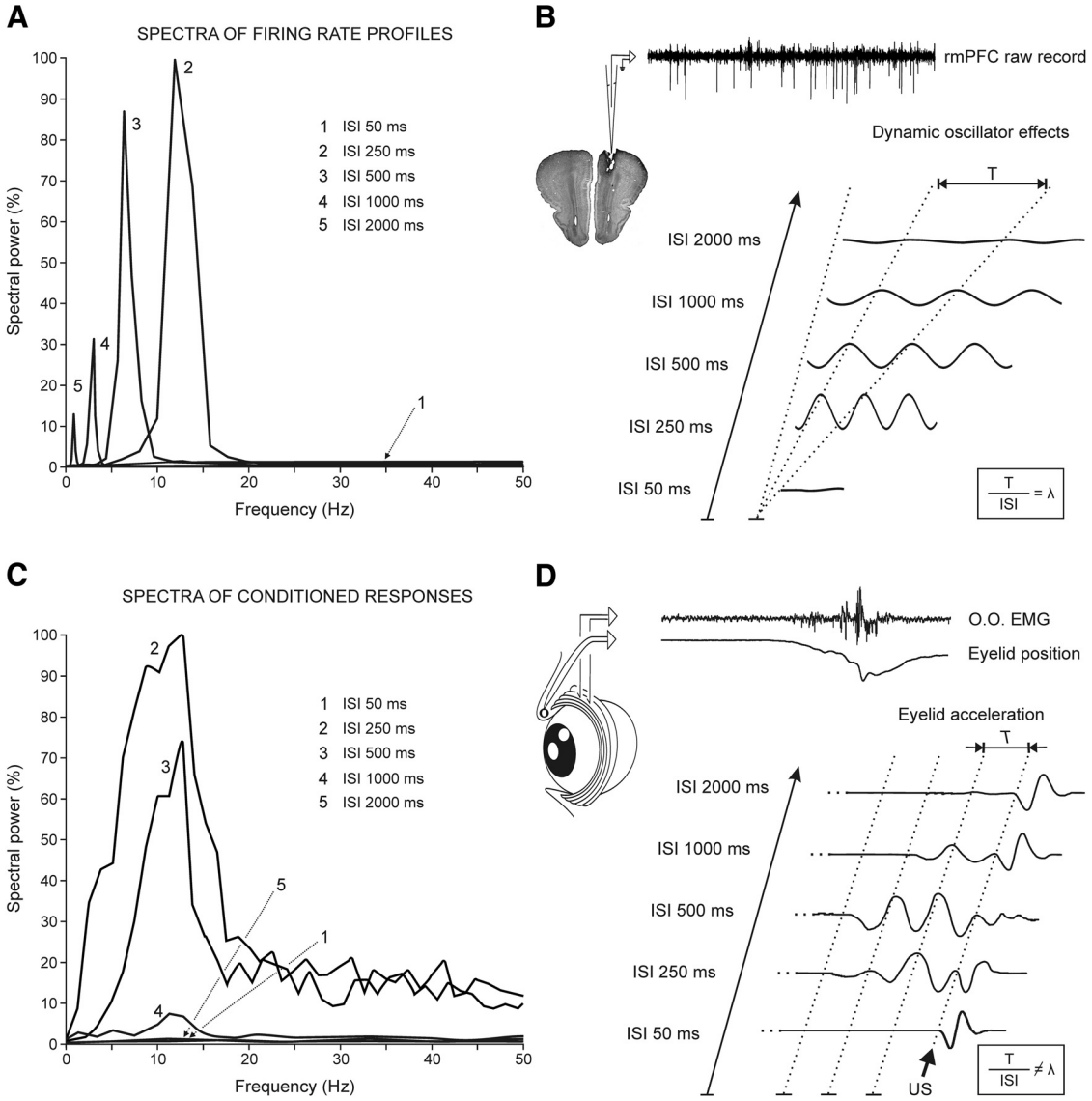

Figure 7. Comparative analysis of the frequency domains for eyelid CRs and for the firing activities of rmPFC neurons during classical conditioning. ***A***, Mean spectral powers computed from the 10 curves fitted to the dominant peaks present in the firing rates of rmPFC neurons. The five illustrated spectral powers correspond to the following CS-US intervals: 50 ms (1), 250 ms (2), 500 ms (3), 1000 ms (4), and 2000 ms (5). The 100% value for the illustrated spectral powers corresponds to 0.6×10^4 (spike/s)^2. ***B***, Representation of waveforms corresponding to the five CS-US intervals included in this study. Note that waveforms depend (in amplitude and frequency) on CS-US intervals, and *T* periods increase with the duration of interstimulus interval (ISI), consistent with a constant $\lambda = \frac{T}{ISI} \approx 0.33$. ***C***, Mean spectral powers of conditioned eyelid responses recorded with the five CS-US intervals indicated in ***A***. Each mean spectral power was obtained from ≥10 acceleration profiles recorded in ≥2 rabbits. The 100% value for the illustrated spectral powers corresponded to 0.3×10^7 (deg/s^2)^2. The code numbers (1–5) are as in ***A***. ***D***, Representation of eyelid acceleration profiles collected from the five CS-US intervals. The beginning of US presentation is indicated. Note that the periods of the accelerations do not depend on CS-US intervals $\left(\text{i.e., } \frac{T}{ISI} \neq \lambda\right)$.

process of reaching a target in a given time window with the help of a fixed-frequency neuronal oscillating machinery (Domingo et al., 1997).

Because the eyelid is load free and facial motoneurons receive no proprioceptive feedback signals from the orbicularis muscle (Porter et al., 1989; Trigo et al., 1999), it could be suggested that the oscillatory behavior of the eyelid is the result of the activity of the neuronal mechanisms controlling it. In fact, it has been shown recently in cats and rats that lid oscillations are an inherent rhythmical property of facial motoneurons innervating the orbicularis oculi muscle (Magariños-Ascone et al., 1999; Trigo et al., 1999). In addition, a noticeable oscillatory behavior has been reported in cat pericruciate cortex neurons during classical eyeblink conditioning (Aou et al., 1992) and in cat cerebellar interpositus neurons during reflexively evoked and classically conditioned eyelid responses (Gruart and Delgado-García, 1994; Jiménez-Díaz et al., 2004). These data suggested that the eyelid motor system could be controlled by a central neural oscillator tuned to the inertial and viscoelastic needs of moving appendages. However, the present results indicate that the oscillatory properties of the rmPFC reported here are not related to the proper generation of eyelid CRs, a point that is discussed below.

Putative role of the oscillatory properties of rmPFC neurons as a timing device for CS-US association

Comparing our results with similar unitary recording and/or lesion studies performed in more caudal or dorsolateral prefrontal areas, which are thought to determine the increasing relevance of

CS presentations or that present firing activities that persist during the whole CS-US interval (Weible et al., 2000, 2003, 2006; Weiss and Disterhoft, 2011; Siegel et al., 2012; Siegel and Mauk, 2013), we can suggest a differential role of rmPFC neurons in the acquisition of classical eyeblink conditioning. The possibility that the persistent neural activity recorded in both dorsolateral and caudomedial PFC during the CS-US interval could be generated by fast-spiking interneurons, but not by projecting pyramidal prefrontal neurons (Povysheva et al., 2006), should be discarded because of the low percentage (6–8%) of putative interneurons present in the rmPFC (Barthó et al., 2004; Insel and Barnes, 2015). Nevertheless, visual observation of neural discharge rates illustrated in those reports (Fig. 4*A* in Siegel et al., 2012; Fig. 4 in Siegel and Mauk, 2013; Fig. 4*A–C* in Hattori et al., 2014) indicates the presence of evident peaks and valleys in the illustrated firing profiles. Therefore, a spectral analysis of those firing profiles could perhaps present dominant frequencies similar to those reported here.

In contrast, the discharge rate of rmPFC neurons recorded in the present study was dependent on the activity of a variable oscillator that enabled the determination of CS-US intervals in an optimal range of 250–500 ms by the successive activation of three different groups of prefrontal units. Because of their spike profiles and firing properties, rmPFC neurons recorded here are similar to the rmPFC pyramidal cells described by Leal-Campanario et al. (2013). These pyramidal neurons were identified by their antidromic and/or synaptic activation from the mediodorsal thalamic nucleus. As described previously (Herry et al., 1999; Leal-Campanario et al., 2013) and confirmed by the present results, the activity of recorded rmPFC neurons during CS-US intervals was not significantly related to the percentage of CRs and/or to the area of the rectified EMG activity of the orbicularis oculi muscle.

The rmPFC of subprimates is homologous to the prefrontal orbital area of primates. Both of them receive a well defined projection from the medial half of the thalamic mediodorsal nucleus (Benjamin et al., 1978; Ray et al., 1992; Kronforst-Collins and Disterhoft, 1998; Leal-Campanario et al., 2007). The neurons recorded here are located in the rostral site of area 24 (anterior cingulate cortex) and the rostrodorsal part of area 32 (prelimbic cortex), but not in the area 24c involved in facial expression in monkeys (Buchanan et al., 1994; Morecraft et al., 2001, 2012).

Prefrontal areas 24 and 32 project to the caudate nucleus, the claustrum, and other striated areas from which prefrontal commands can reach many different sensorimotor cortical and subcortical centers (Buchanan et al., 1994; Kronforst-Collins and Disterhoft, 1998; Fuster, 2001). In addition to the mediodorsal thalamic nucleus, rmPFC areas also project to other midline thalamic nuclei, regulating unspecific sensory inputs related to attentive processes and to the presence of novel sensory stimuli. Finally, PFC neurons project to different midbrain centers, including the substantia nigra pars reticulata, which is involved in movement initiation and coordination, and the pontine nuclei projecting heavily to the cerebellar cortex and nuclei (Basso and Evinger, 1996; Basso et al., 1996; Kronforst-Collins and Disterhoft, 1998; Siegel et al., 2012). However, the peculiar discharge rates of rmPFC neurons described in this study seem to be more related to the cognitive components of classical conditioning than to the generation of conditioned eyeblinks. Neural activities shown here could reach other cortical areas more directly involved in nonmotor aspects of this type of associative learning. For example, during trace eyeblink conditioning in the rabbit, caudal areas of the anterior cingulate cortex are involved in the salience or relevance of CS presentations (Weible et al., 2003). In addition, caudal mPFC and dorsolateral PFC neurons present firing activities that persist during the CS-US interval in trace conditioning paradigms, helping in the generation of timed conditioned eyeblinks (Weiss and Disterhoft, 2011; Siegel and Mauk, 2013). Moreover, rmPFC neural signals can reach the hippocampus either directly or across the thalamic reuniens nucleus (McKenna and Vertes, 2004).

In summary, these results provide new evidence on the presence in the rmPFC of a variable oscillator that helps to determine time intervals during associative learning tasks. This neural oscillator seems to be particularly adapted to determine CS-US intervals in the range of 250–500 ms, the optimal values for the proper generation of conditioned nictitating membrane and eyelid responses in behaving rabbits and cats (Gormezano et al., 1983; Domingo et al., 1997; Gruart et al., 2000).

References

Aou S, Woody CD, Birt D (1992) Changes in the activity of units of the cat motor cortex with rapid conditioning and extinction of a compound eye blink movement. J Neurosci 12:549–559. Medline

Barthó P, Hirase H, Monconduit L, Zugaro M, Harris KD, Buzsáki G (2004) Characterization of neocortical principal cells and interneurons by network interactions and extracellular features. J Neurophysiol 92:600–608. CrossRef Medline

Basso MA, Evinger C (1996) An explanation for reflex blink hyperexcitability in Parkinson's disease. II. Nucleus raphe magnus. J Neurosci 16:7318–7330. Medline

Basso MA, Powers AS, Evinger C (1996) An explanation for reflex blink hyperexcitability in Parkinson's disease. I. Superior colliculus. J Neurosci 16:7308–7317. Medline

Benjamin RM, Jackson JC, Golden GT (1978) Cortical projections of the thalamic mediodorsal nucleus in the rabbit. Brain Res 141:251–265. CrossRef Medline

Berthier NE (1992) Muscle activity during unconditioned and conditioned eye blinks in the rabbit. Behav Brain Res 48:21–28. CrossRef Medline

Buchanan SL, Thompson RH, Maxwell BL, Powell DA (1994) Efferent connections of the medial prefrontal cortex in the rabbit. Exp Brain Res 100:469–483. CrossRef Medline

Caro-Martín CR, Sánchez-Campusano R, Delgado-García JM, Leal-Campanario R, Gruart A (2014) Spike sorting and firing rate distribution of prefrontal cortex neurons during delayed eyeblink conditioning. Acta Physiologica 52:41–42.

Caro-Martín CR, Leal-Campanario R, Sánchez-Campusano R, Delgado-García JM, Gruart A (2015) A variable oscillator underlies the measurement of time intervals in the medial prefrontal cortex during classical eyeblink conditioning in rabbits. Soc Neurosci Abstr 41:3534.

Clark GA, McCormick DA, Lavond DG, Thompson RF (1984) Effects of lesions of cerebellar nuclei on conditioned behavioral and hippocampal neuronal responses. Brain Res 291:125–136. CrossRef Medline

Dégenètais E, Thierry AM, Glowinski J, Gioanni Y (2002) Electrophysiological properties of pyramidal neurons in the rat prefrontal cortex: an in vivo intracellular recording study. Cereb Cortex 12:1–16. CrossRef Medline

Domingo JA, Gruart A, Delgado-García JM (1997) Quantal organization of reflex and conditioned eyelid responses. J Neurophysiol 78:2518–2530. Medline

Eichenbaum H (2014) Time cells in the hippocampus: a new dimension for mapping memories. Nat Rev Neurosci 15:732–744. CrossRef Medline

Elble RJ (1996) Central mechanisms of tremor. J Clin Neurophysiol 13:133–144. CrossRef Medline

Evinger C, Shaw MD, Peck CK, Manning KA, Baker R (1984) Blinking and associated eye movements in humans, guinea pigs, and rabbits. J Neurophysiol 52:323–339. Medline

Fuster JM (2001) The prefrontal cortex–an update: time is of the essence. Neuron 30:319–333. CrossRef Medline

Fuster JM (2008) The prefrontal cortex, Ed 4. London: Academic.

Girgis M, Shih-Chang W (1981) A new stereotaxic atlas of the rabbit brain. St. Louis: Warren H. Green.

Gormezano I, Kehoe EJ, Marshall BS (1983) Twenty years of classical conditioning research with the rabbit. Prog Psychobiol Physiol Psychol 10:197–275.

Gruart A, Delgado-García JM (1994) Discharge of identified deep cerebellar nuclei neurons related to eye blinks in the alert cat. Neuroscience 61:665–681. CrossRef Medline

Gruart A, Blázquez P, Delgado-García JM (1995) Kinematics of spontaneous, reflex, and conditioned eyelid movements in the alert cat. J Neurophysiol 74:226–248. Medline

Gruart A, Schreurs BG, del Toro ED, Delgado-García JM (2000) Kinetic and frequency-domain properties of reflex and conditioned eyelid responses in the rabbit. J Neurophysiol 83:836–852. Medline

Hattori S, Yoon T, Disterhoft JF, Weiss C (2014) Functional reorganization of a prefrontal cortical network mediating consolidation of trace eyeblink conditioning. J Neurosci 34:1432–1445. CrossRef Medline

Herry C, Vouimba RM, Garcia R (1999) Plasticity in the mediodorsal thalamo-prefrontal cortical transmission in behaving mice. J Neurophysiol 82:2827–2832. Medline

Howard MW, Eichenbaum H (2015) Time and space in the hippocampus. Brain Res 1621:345–354. CrossRef Medline

Insel N, Barnes CA (2015) Differential activation of fast-spiking and regular-firing neuron populations during movement and reward in the dorsal medial frontal cortex. Cereb Cortex 25:2631–2647. CrossRef Medline

Jiménez-Díaz L, Navarro-López Jde D, Gruart A, Delgado-García JM (2004) Role of cerebellar interpositus nucleus in the genesis and control of reflex and conditioned eyelid responses. J Neurosci 24:9138–9145. CrossRef Medline

Koekkoek SK, Den Ouden WL, Perry G, Highstein SM, De Zeeuw CI (2002) Monitoring kinetic and frequency-domain properties of eyelid responses in mice with magnetic distance measurement technique. J Neurophysiol 88:2124–2133. Medline

Kolb B, Pellis S, Robinson TE (2004) Plasticity and functions of the orbital frontal cortex. Brain Cogn 55:104–115. CrossRef Medline

Kronforst-Collins MA, Disterhoft JF (1998) Lesions of the caudal area of rabbit medial prefrontal cortex impair trace eyeblink conditioning. Neurobiol Learn Mem 69:147–162. CrossRef Medline

Leal-Campanario R, Fairén A, Delgado-García JM, Gruart A (2007) Electrical stimulation of the rostral medial prefrontal cortex in rabbits inhibits the expression of conditioned eyelid responses but not their acquisition. Proc Natl Acad Sci U S A 104:11459–11464. CrossRef Medline

Leal-Campanario R, Delgado-García JM, Gruart A (2013) The rostral medial prefrontal cortex regulates the expression of conditioned eyelid responses in behaving rabbits. J Neurosci 33:4378–4386. CrossRef Medline

Llinás RR (1991) The noncontinuous nature of movement execution. In: Motor control: concepts and issues (Humphrey DR, Freund HJ, eds), pp 223–242. New York: Wiley.

Louis ED (2014) Essential tremor: from bedside to bench and back to bedside. Curr Opin Neurol 27:461–467. CrossRef Medline

Magariños-Ascone C, Núñez A, Delgado-García JM (1999) Different discharge properties of dorsolateral facial nucleus motoneurons: intracellular in vitro recordings. Neuroscience 94:879–886. CrossRef Medline

Marquis DG, Porter JM (1939) Differential characteristics of conditioned eyelid responses established by reflex and voluntary reinforcement. J Exp Psychol 24:347–365. CrossRef

McKenna JT, Vertes RP (2004) Afferent projections to nucleus reuniens of the thalamus. J Comp Neurol 480:115–142. CrossRef Medline

Morecraft RJ, Louie JL, Herrick JL, Stilwell-Morecraft KS (2001) Cortical innervation of the facial nucleus in the non-human primate: a new interpretation of the effects of stroke and related subtotal brain trauma on the muscles of facial expression. Brain 124:176–208. CrossRef Medline

Morecraft RJ, Stilwell-Morecraft KS, Cipolloni PB, Ge J, McNeal DW, Pandya DN (2012) Cytoarchitecture and cortical connections of the anterior cingulate and adjacent somatomotor fields in the rhesus monkey. Brain Res Bull 87:457–497. CrossRef Medline

Múnera A, Gruart A, Muñoz MD, Fernández-Mas R, Delgado-García JM (2001) Hippocampal pyramidal cell activity encodes conditioned stimulus predictive value during classical conditioning in alert cats. J Neurophysiol 86:2571–2582. Medline

Oswald B, Knuckley B, Mahan K, Sanders C, Powell DA (2006) Prefrontal control of trace versus delay eyeblink conditioning: role of the unconditioned stimulus in rabbits (Oryctolaguscuniculus). Behav Neurosci 120:1033–1042. CrossRef Medline

Pacheco-Calderón R, Carretero-Guillén A, Delgado-García JM, Gruart A (2012) Red nucleus neurons actively contribute to the acquisition of classically conditioned eyelid responses in rabbits. J Neurosci 32:12129–12143. CrossRef Medline

Paraskevopoulou SE, Barsakcioglu DY, Saberi MR, Eftekhar A, Constandinou TG (2013) Feature extraction using first and second derivative extrema (FSDE) for real time and hardware-efficient spike sorting. J Neurosci Methods 215:29–37. CrossRef Medline

Park YG, Park HY, Lee CJ, Choi S, Jo S, Choi H, Kim YH, Shin HS, Llinas RR, Kim D (2010) Ca(V)3.1 is a tremor rhythm pacemaker in the inferior olive. Proc Natl Acad Sci U S A 107:10731–10736. CrossRef Medline

Porras-García E, Sánchez-Campusano R, Martínez-Vargas D, Domínguez-del-Toro E, Cendelín J, Vozeh F, Delgado-García JM (2010) Behavioral characteristics, associative learning capabilities, and dynamic association mapping in an animal model of cerebellar degeneration. J Neurophysiol 104:346–365. CrossRef Medline

Porter JD, Burns LA, May PJ (1989) Morphological substrate for eyelid movements: innervation and structure of primate levator palpebrae superioris and orbicularis oculi muscle. J Comp Neurol 287:64–81. CrossRef Medline

Povysheva NV, Gonzalez-Burgos G, Zaitsev AV, Kröner S, Barrionuevo G, Lewis DA, Krimer LS (2006) Properties of excitatory synaptic responses in fast-spiking interneurons and pyramidal cells from monkey and rat prefrontal cortex. Cereb Cortex 16:541–552. Medline

Powell DA, Churchwell J, Burriss L (2005) Medial prefrontal lesions and Pavlovian eyeblink and heart rate conditioning: effects of partial reinforcement on delay and trace conditioning in rabbits (Oryctolaguscuniculus). Behav Neurosci 119:180–189. CrossRef Medline

Ray JP, Russchen FT, Fuller TA, Price JL (1992) Sources of presumptive glutamatergic/aspartatergic afferents to the mediodorsal nucleus of the thalamus in the rat. J Comp Neurol 320:435–456. CrossRef Medline

Sánchez-Campusano R, Gruart A, Delgado-García JM (2007) The cerebellar interpositus nucleus and the dynamic control of learned motor responses. J Neurosci 27:6620–6632. CrossRef Medline

Shek JW, Wen GY, Wisniewski HM (1986) Atlas of the rabbit brain and spinal cord. Zurich: Karger.

Siegel JJ, Mauk MD (2013) Persistent activity in prefrontal cortex during trace eyelid conditioning: dissociating responses that reflect cerebellar output from those that do not. J Neurosci 33:15272–15284. CrossRef Medline

Siegel JJ, Kalmbach B, Chitwood RA, Mauk MD (2012) Persistent activity in a cortical-to-subcortical circuit: bridging the temporal gap in trace eyelid conditioning. J Neurophysiol 107:50–64. CrossRef Medline

Su CK, Chiang CH, Lee CM, Fan YP, Ho CM, Shyu LY (2013) Computational solution of spike overlapping using data-based subtraction algorithms to resolve synchronous sympathetic nerve discharge. Front Comp Neurosci 7:149. CrossRef Medline

Takehara-Nishiuchi K, Kawahara S, Kirino Y (2005) NMDA receptor-dependent processes in the medial prefrontal cortex are important for acquisition and the early stage of consolidation during trace, but not delay eyeblink conditioning. Learn Mem 12:606–614. CrossRef Medline

Trigo JA, Gruart A, Delgado-García JM (1999) Discharge properties of abducens, accessory abducens, and orbicularis oculi motoneurons during unconditioned and conditioned eye blinks in the alert cat. J Neurophysiol 81:1666–1684. Medline

Volkmann J, Joliot M, Mogilner A, Ioannides AA, Lado F, Fazzini E, Ribary U, Llinás R (1996) Central motor loop oscillations in parkinsonian resting tremor revealed by magnetoencephalography. Neurology 46:1359–1370. CrossRef Medline

Weible AP, McEchron MD, Disterhoft JF (2000) Cortical involvement in acquisition and extinction of trace eyeblink conditioning. Behav Neurosci 114:1058–1067. Medline

Weible AP, Weiss C, Disterhoft JF (2003) Activity profiles of single neurons in caudal anterior cingulate cortex during trace eyeblink conditioning in the rabbit. J Neurophysiol 90:599–612. CrossRef Medline

Weible AP, O'Reilly JA, Weiss C, Disterhoft JF (2006) Comparisons of dorsal and ventral hippocampus cornu ammonis region 1 pyramidal neuron activity during trace eye-blink conditioning in the rabbit. Neuroscience 141:1123–1137. Medline

Weiss C, Disterhoft JF (2011) Exploring prefrontal cortical memory mechanisms with eyeblink conditioning. Behav Neurosci 125:318–326. CrossRef Medline

Welsh JP (1992) Changes in the motor pattern of learned and unlearned responses following cerebellar lesions: a kinematic analysis of the nictitating membrane reflex. Neuroscience 47:1–19. CrossRef Medline

Wessberg J, Vallbo AB (1995) Coding of pulsatile motor output by human muscle afferents during slow finger movement. J Physiol 485:271–282. CrossRef Medline